How close are integrable and nonintegrable models: A parametric case study based on the Salerno model

Thudiyangal Mithun,[1] Aleksandra Maluckov,[2] Ana Mančić,[3] Avinash Khare,[4] and Panayotis G. Kevrekidis[1]
[1]*Department of Mathematics and Statistics, University of Massachusetts, Amherst, Massachusetts 01003-4515, USA*
[2]*COHERENCE, Vinča Institute of Nuclear Sciences, National Institute of the Republic of Serbia, University of Belgrade, P.O.B. 522, 11001 Belgrade, Republic of Serbia*
[3]*COHERENCE, Department of Physics, Faculty of Sciences and Mathematics, University of Niš, P.O.B. 224, 18000 Niš, Serbia*
[4]*Department of Physics, Savitribai Phule Pune University, Pune 411007, India*

(Received 10 October 2022; accepted 9 January 2023; published 7 February 2023)

In the present work we revisit the Salerno model as a prototypical system that interpolates between a well-known integrable system (the Ablowitz-Ladik lattice) and an experimentally tractable, nonintegrable one (the discrete nonlinear Schrödinger model). The question we ask is, for "generic" initial data, how close are the integrable to the nonintegrable models? Our more precise formulation of this question is, How well is the constancy of formerly conserved quantities preserved in the nonintegrable case? Upon examining this, we find that even slight deviations from integrability can be sensitively felt by measuring these formerly conserved quantities in the case of the Salerno model. However, given that the knowledge of these quantities requires a deep physical and mathematical analysis of the system, we seek a more "generic" diagnostic towards a manifestation of integrability breaking. We argue, based on our Salerno model computations, that the full spectrum of Lyapunov exponents could be a sensitive diagnostic to that effect.

DOI: 10.1103/PhysRevE.107.024202

I. INTRODUCTION

The topic of nonlinear dynamical lattices and energy localization in them has been prevalent in a large array of studies over the past few decades [1,2]. Indeed, since the proposal of intrinsic localized modes in anharmonic crystals [3,4], there has been an ever-expanding range of disciplines where relevant states and their implications are being identified, explored, and dynamically exploited [5]. Among the numerous associated examples, one can list arrays of waveguides in nonlinear optics [6], Bose-Einstein condensates in optical lattices [7], manipulation of localization in micromechanical oscillator arrays [8], granular crystals in materials science [9,10], lattices of electrical circuits [11], and many others, including layered antiferromagnetic crystals [12,13], Josephson-junction ladders [14,15], or dynamical models of the DNA double strand [16].

In many of these works, part of the emphasis has been on localization and nonlinear wave structures [2,5,17,18]. Important associated questions involve the existence, dynamical stability, and nonlinear dynamics of the relevant wave forms. A parallel line of activity that has also been central from early on has been that of potential long-time ergodicity of the nonlinear lattice dynamical systems [1,19]. In the latter there have been significant developments in recent times, where computational resources have enabled far longer time simulations of different classes of such systems [20–22] and the development of novel systems that are more straightforward to simulate over long times [23]. Interestingly, the birth of the scientific field examining nonlinear wave (solitonic) structures has been strongly connected with such ergodicity-related quests [24,25].

The concept of integrability [26,27] is one that is central to both of the above directions of study. On the one hand, the development of the inverse scattering transform and the identification of solitonic structures for a number of these equations has been a key development in nonlinear wave dynamics [26,27], while on the other hand, the infinite conservation laws and associated constraints that such systems impose on the dynamics have significant bearings on the ability of the system to explore its phase space. Moreover, often integrability has been a "helpful hand" towards trying to understand the dynamics of weakly nonintegrable systems through approaches involving perturbation theory [28]. Here, often an effective adiabaticity assumption is implied, i.e., that the structures of the integrable (or analytically tractable) limit are preserved but their features (e.g., amplitude, width, speed, etc.) are modified and dynamically driven by the nonintegrable perturbations imposed. Indeed, this proximity has been recently also of substantial mathematical interest through, e.g., the works of [29,30].

In the present work, it is our intention to return to the exploration of this topic of the effective proximity of integrable and weakly nonintegrable systems. Indeed, we leverage here a different perspective from those of works such as [29,30] which focus on the (small) amplitude of the solution to gauge the relevant proximity. Rather, we deploy a comparison on the basis of conservation laws of the original integrable system (see also the work of [31]). Our aim is to explore more broadly the phase space of the lattice dynamical system

and its constraints as we depart from the integrable limit. As our platform of choice, we will utilize the well-known so-called Salerno model [32], given its natural interpolation between the well-established integrable variant of the nonlinear Schrödinger equation (the so-called Ablowitz-Ladik, AL, limit) [33,34] and the nonintegrable so-called DNLS (discrete nonlinear Schrödinger) equation [18]. The advantage of this system is the availability of a homotopic parameter interpolating between these models and allowing us to explore the departure from the integrable limit.

Our tool of choice will be the usage of conservation laws of the AL limit initially. We will explore how "sensitive" these are as probes of the breaking of integrability. We will find that indeed "former conservation laws" will be very sensitive to departures from the relevant limit. However, a disadvantage of this approach is that it requires a deep mathematical or physical (or both) knowledge of the concrete features of the system at hand. In that light, it is desirable to have a more general toolbox that is somewhat "system independent" in order to (sensitively) probe such departures from the integrable limit. In that vein, we explore the maximal Lyapunov exponent and, indeed, the full Lyapunov spectrum of the system of interest that can be generally computed [35–37]. We find that this represents a very efficient tool for detecting the number of available conservation laws and hence integrability of the system, indeed, one that we expect in the future to be amenable to efficient computation, e.g., via machine-learning techniques.

Our presentation will be structured as follows. In Sec. II we present the model of interest and its associated conservation laws that we will probe both in the integrable limit and systematically as we depart from that limit. In Sec. III we present our results for the corresponding conservation laws and their long-time dynamics. In Sec. IV we discuss the computation of the Lyapunov exponent spectrum, regarding both the maximal Lyapunov exponent and the full spectrum, and present associated numerical results. In Sec. V we summarize our findings and present our conclusions, as well as a number of directions for future study.

II. MODEL DESCRIPTION

The equation that we will consider in the present study involves the well-established Salerno model [32], which interpolates between the AL and the DNLS limits. The relevant dynamical equation reads

$$i\frac{d\psi_n}{dt} = (1+\mu|\psi_n|^2)(\psi_{n+1}+\psi_{n-1})+\gamma|\psi_n|^2\psi_n. \tag{1}$$

This system has been a natural playground for the usage of perturbation theory methods off of the integrable limit [38], for the examination of the delicate issue of mobility in lattice dynamical systems [39], for the exploration of collisions [31], and for the analysis of statistical mechanical properties of nonlinear lattices [40], among many others.

The AL model is well known to be integrable via the inverse scattering transform [34]. This implies the existence of an infinite number of conserved quantities considered, e.g., in the work of [41], while the nonintegrable DNLS limit is characterized solely by two integrals of motion, namely, the energy and the (squared) l^2 norm of the field. Indeed, the

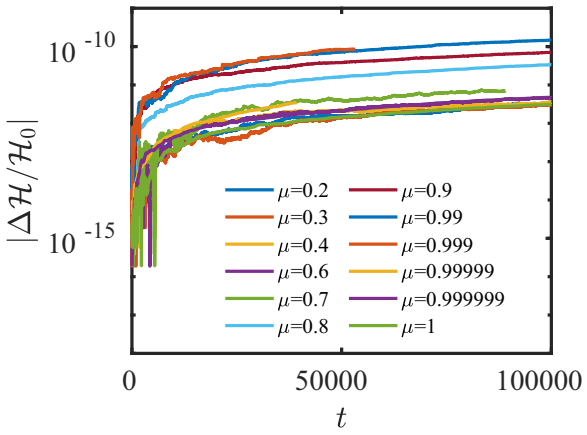

FIG. 1. The relative error of energy $\Delta\mathcal{H}/\mathcal{H}_0$, $\Delta\mathcal{H} = \mathcal{H}(t) - \mathcal{H}_0$, for different μ vs time for an end time of 100 000. A numerical Runge-Kutta (RK) procedure with adaptive step is applied. The values of μ are shown in the figure, while $N = 100$. During the calculations in order for the code to run in the area above $\mu = 0.9$, the initial time step dt was changed from 0.0001 to 0.000 001. Note that this is only the initial parameter for the adaptive step numerical method. Some of the relevant computations have been stopped at shorter times (for reasons that have to do with error tolerances applied to these long runs).

Salerno model inherits these two conservation laws. More specifically, regardless of the limits, Eq. (1) can be characterized by two conserved quantities: the (squared) norm $\mathcal{A}$ and the Hamiltonian $\mathcal{H}$, i.e., the energy of the model [38,42] in the form

$$\mathcal{A} = \sum_{n=1}^{N}\mathcal{A}_n, \quad \mathcal{A}_n = \frac{1}{\mu}\ln|1+\mu|\psi_n|^2|$$
$$\mathcal{H} = \sum_{n=1}^{N}\left[-\frac{\gamma}{\mu}\mathcal{A}_n + \psi_n\psi_{n+1}^* + \psi_n^*\psi_{n+1} + \frac{\gamma}{\mu}|\psi_n|^2\right], \tag{2}$$

where N is the total number of lattice nodes, and periodic boundary conditions are used. Notice that the latter will be an important point, especially when we consider finite, small-size lattices, as integrability of the AL model is preserved in the case of periodic boundary conditions, although other types of integrable boundary conditions may also exist [43]. It is also relevant to point out that in the DNLS limit of $\mu \to 0$, application of l'Hospital (or a Taylor expansion in μ) leads to the first conserved quantity turning into the (squared) l^2 norm.

The dynamical equations of the Salerno model in the form of Eq. (1) can be derived from the Hamiltonian $\mathcal{H}$ according to

$$\frac{d\psi_n}{dt} = \{\mathcal{H}, \psi_n\}, \tag{3}$$

with respect to the canonically conjugated pairs of variables ψ_n and ψ_n^* defining the deformed Poisson brackets [44]:

$$\{\psi_n, \psi_m^*\} = i(1+\mu|\psi_n|^2)\delta_{nm}, \quad \{\psi_n, \psi_m\} = \{\psi_n^*, \psi_m^*\} = 0. \tag{4}$$

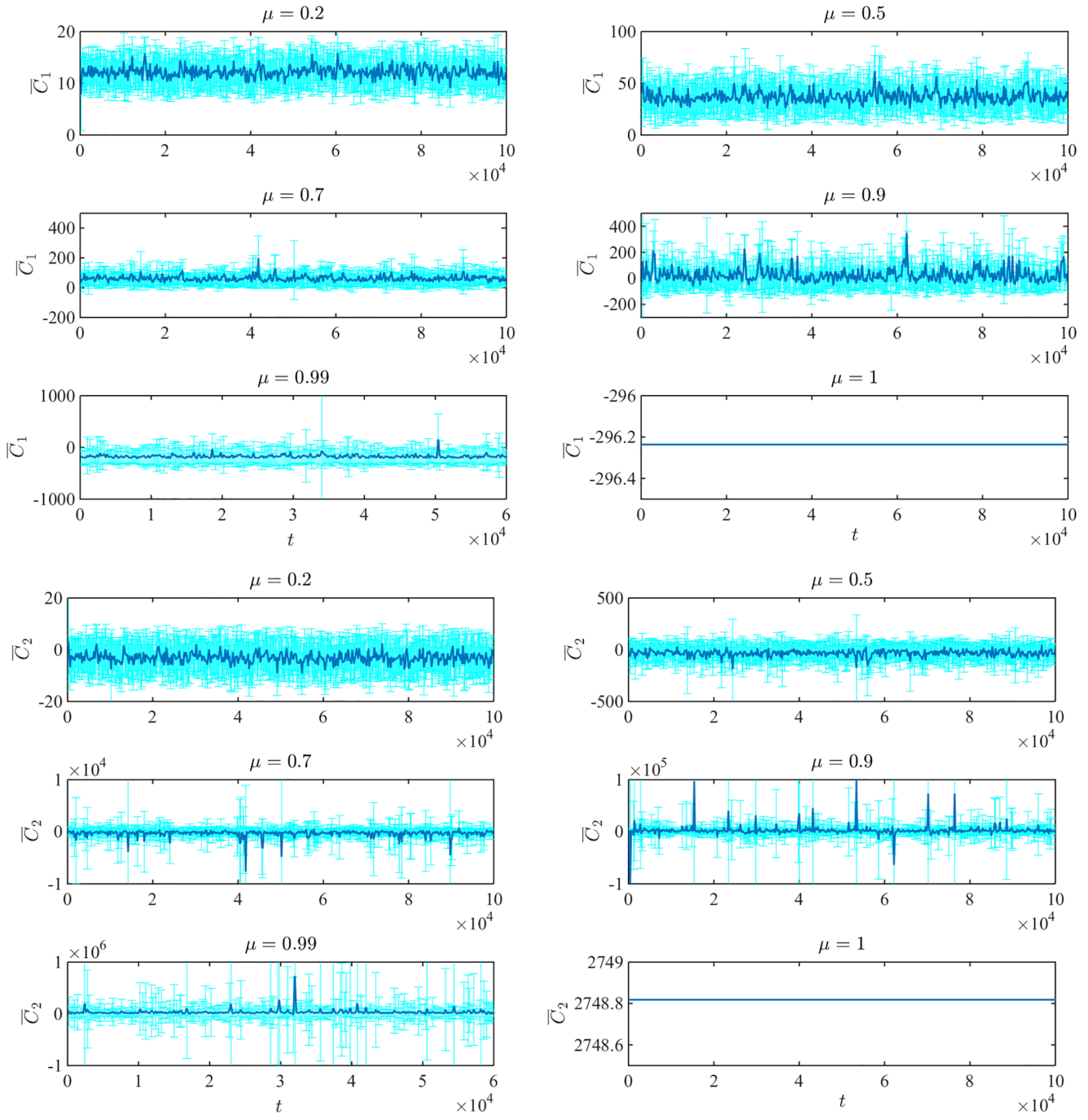

FIG. 2. The average over the successive $\Delta t = 100$ a.u. (a.u. stands for arbitrary time units) real parts of the complex moments, $\overline{C}_1$ and $\overline{C}_2$ (i.e., the quantities that are conserved in the AL limit but not away from it) vs μ. The moments are numerically calculated at each selected time step using the equation of motion (1). Initially, at $t = 0$, $N = 100$ lattice nodes at each μ are excited by the plane wave with parameters $a \equiv \mathcal{A}/N = 1.5$ and $h = \mathcal{H}/N = 3$, to which a complex random perturbation in space is added by means of a numerical uniform random number generator. The set of random numbers from the interval between $(-0.5, 0.5)$ is used, while the strength of the corresponding perturbation is 0.001. Bars denote the standard deviation around the mean value taken over a time interval of $t = 100$ along the whole propagation time. The values of μ are specified in the plot.

Among the infinite conservation laws of the AL limit, the two that we will focus on observing here are [41]

$$C_1 = -\mu \sum_n \psi_n^* \psi_{n-1}$$

$$C_2 = -\mu \sum_n \psi_n^* \psi_{n-2} \left[1 + \mu |\psi_{n-1}|^2 + \frac{1}{2} (\psi_n^* \psi_{n-1})^2 \right]. \quad (5)$$

These will be our monitored quantities (that, as we will see, will be quite informative) and which, in the following, will be denoted as moments. In general they are complex quantities. Therefore we considered their real and the imaginary parts, as well as the corresponding modulus.

It is relevant to point out that C_1 is often thought of as a discrete version of the momentum, yet C_2 does not have an

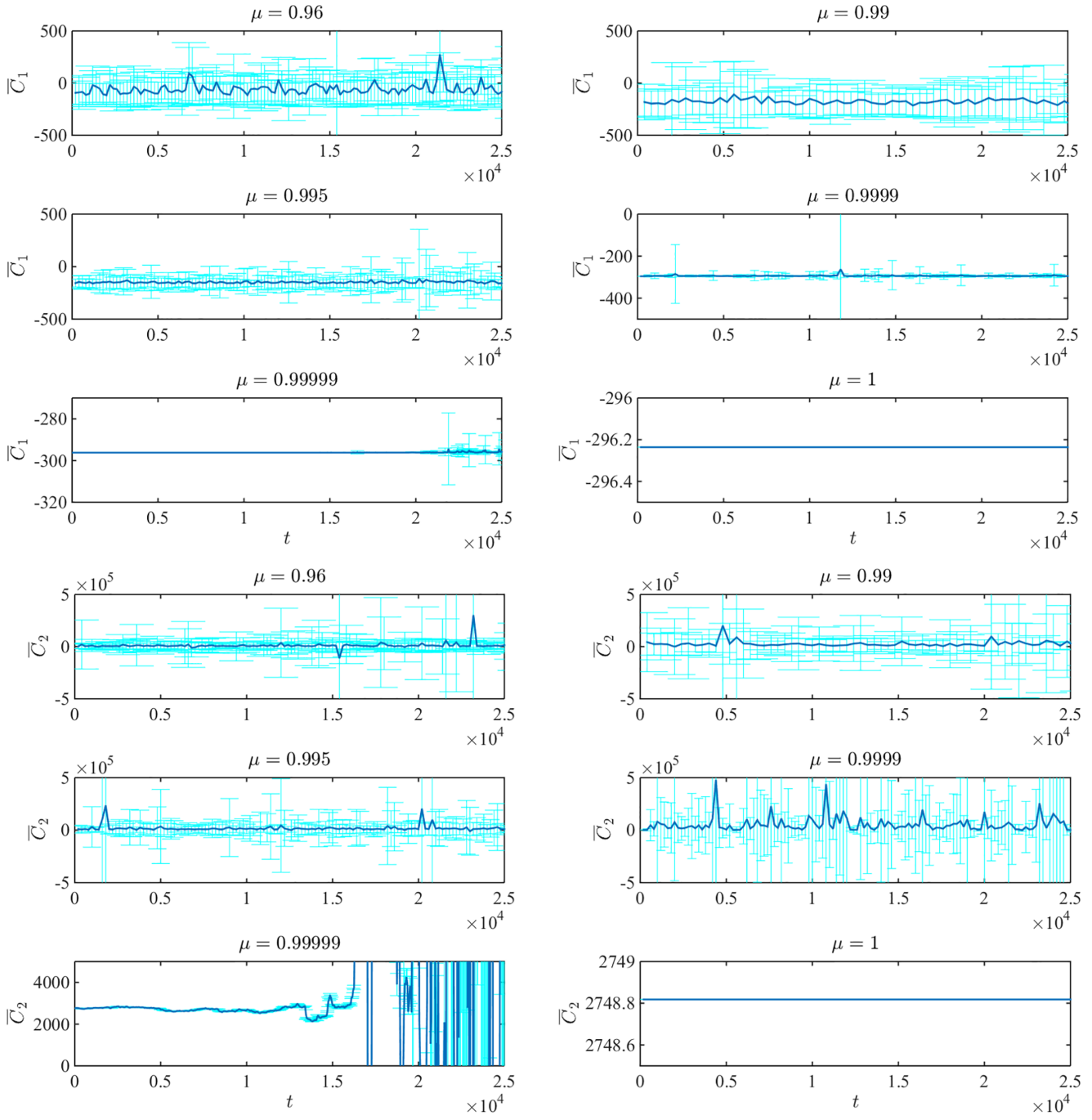

FIG. 3. Here we separately show the behavior of the same moments as in Fig. 2, namely, $\overline{C}_1$ (first three rows) and $\overline{C}_2$ (last three rows) for μ very close to the integrability limit. The features and initialization of these runs are similar to those of the previous figure.

immediate interpretation at a physical level. As an additional relevant remark, the moment C_1 is not sufficient in order to showcase the integrable limit here, as, for instance, it is still conserved as a quantity in the linear limit of $\mu = \gamma = 0$ (not considered in detail herein). On the other hand, the quantity C_2 is strictly conserved in the AL integrable case only, and hence the combination of these two moments should be able to provide us a clearer signature associated with the integrable limit in what follows.

III. COMPUTATION OF CONSERVATION LAWS

In presenting our results, we start with the aforementioned conserved quantities of Eq. (1). Here we gradually deviate from the AL limit of $\mu = 1$ while numerically solving Eq. (1) using an explicit Runge-Kutta algorithm of order 8 [46–48]. The initial conditions are plane waves (motivated by the earlier thermodynamic study of the model in Ref. [40]) $\psi_n = (\sqrt{a} + V\xi_n)\exp[i(\phi_n + V\eta_n)]$ with random phases $\phi_n = n \cdot \arccos[1/(2\,a)\,(h - \gamma/\mu^2 \cdot \ln(1 + \mu\,a) + (\gamma/\mu)a)]$, where

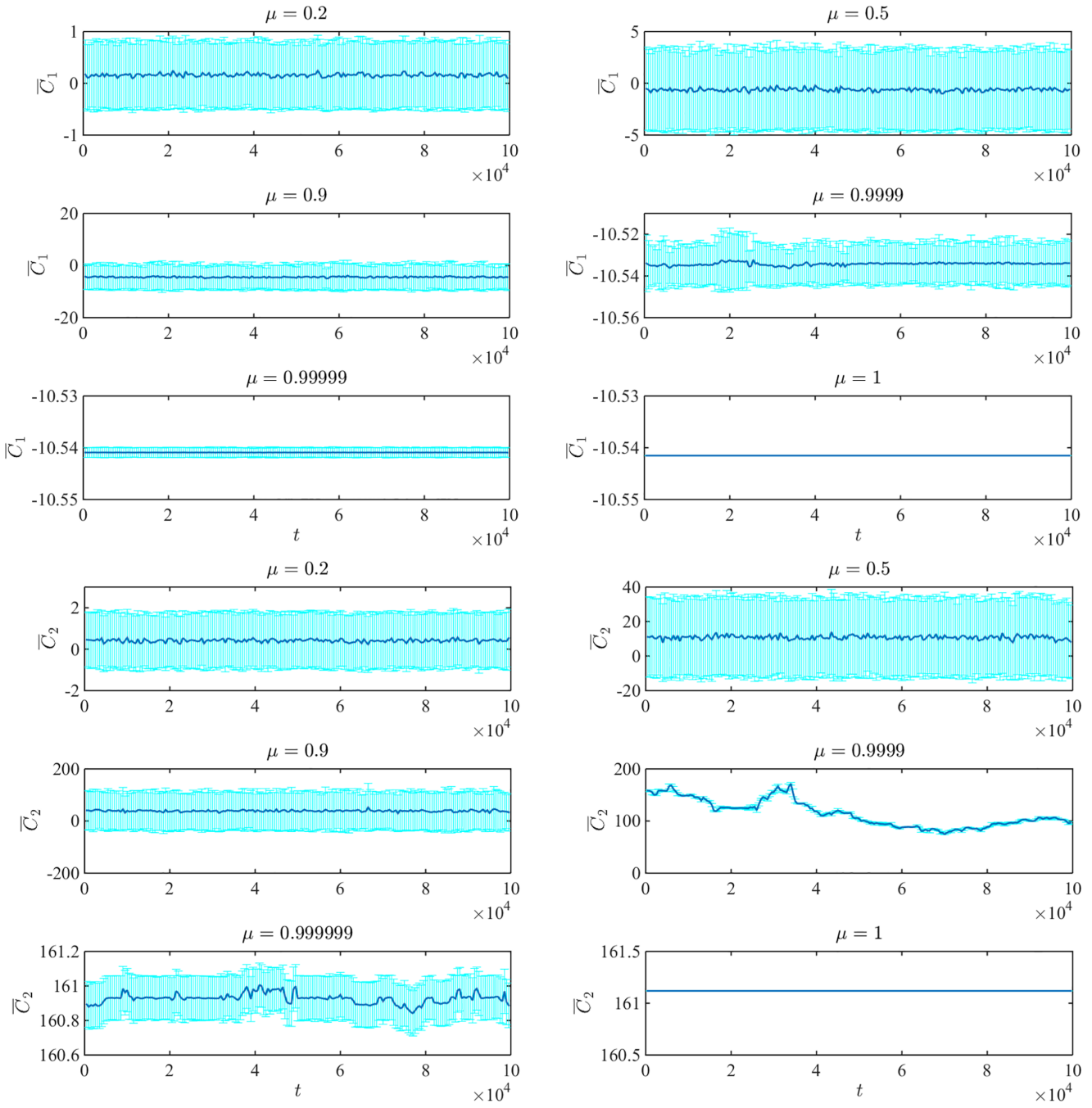

FIG. 4. Here we present the same moment information as in the previous figure but for $N = 5$.

η and ξ are random numbers drawn from the uniform distribution of range $(-0.5, 0.5)$, and $V = 0.001$ is a fixed small perturbation parameter. Additionally, $a = \mathcal{A}/N$ and $h = \mathcal{H}/N$. In the process, we trace the evolution of the relative norm and energy error, $|\frac{\mathcal{A}(t)-\mathcal{A}(0)}{\mathcal{A}(0)}|$ and $|\frac{\mathcal{H}(t)-\mathcal{H}(0)}{\mathcal{H}(0)}|$, respectively, and show a typical example thereof in Fig. 1. It can be seen that the energy is extremely well conserved, with a relative error below 10^{-10} for the simulation horizons reported herein.

Figure 2 shows the time development of the quantities C_1 and C_2 for different values of μ. The important feature to observe in these evolution simulations is that the relevant quantities present substantial time-dependent fluctuations. As may be expected, the general trend of the curves suggests that these fluctuations decrease as μ approaches 1, i.e., the integrable limit. We have further ensured that the above trend persists even for different sizes of the lattice. However, in order to explore how *sensitive* the relevant diagnostics are towards detecting the breaking of integrability, we have also performed the computations of Fig. 3, which are all conducted in the vicinity of the integrable limit. Indeed, the relevant values of μ are within a range of less than 5% variations,

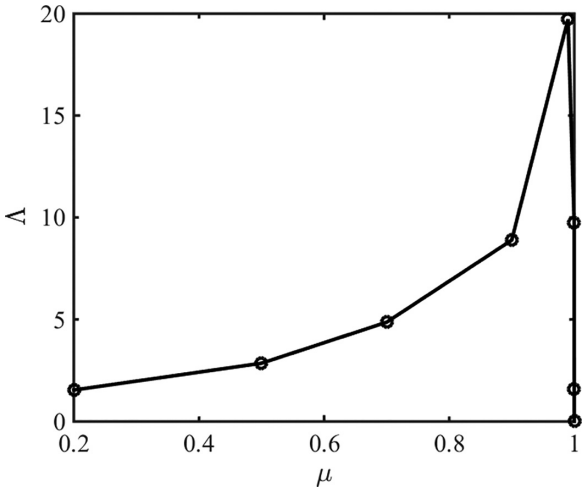

FIG. 5. The mLCE defined by Eq. (7) for different values of μ for fixed $N = 100$, $a = 1.5$, and $h = 3$. Notice the positive value thereof except when we approach the integrable limit $\mu = 1$, when it tends to 0.

which is a typical limit where perturbative considerations might be used [31,44]. Nevertheless, we can observe that in our extended time-horizon evolution dynamics, the relevant quantities present substantial fluctuations (notice the vertical axis scale) even very near the integrable limit. Indeed, they can be observed even for $\mu = 0.999\,99$ in the case of C_2 (although, notably, not in the case of C_1). It is only *at* the integrable limit that all relevant such fluctuations disappear and integrability is retrieved.

An additional aspect that we probe, as the earlier results were for $N = 100$, is how accurate and sensitive these diagnostics may be when N is small, and the limited volume of the phase space may not allow the potential breaking of integrability to be probed. We explore this in Fig. 4 for $N = 5$. This figure, as well as additional tests (not shown), suggest that it may be easier to "mistake" a nonintegrable situation for an integrable one if one uses a very small N, and even more so when one uses a lower moment such as C_1. Already at $N = 5$ deviations from integrability are substantially observable, even quite close to $\mu = 1$, and C_2 turns out to be a more sensitive probe thereof than C_1.

Our conclusion from the above extensive probing of the parameter space is that these "former" conservation laws constitute a *very sensitive* diagnostic feature of the integrability breaking. In fact, such higher-order moments (like C_2) are even more sensitive than lower-order ones (such as C_1). Nevertheless, the examination of such quantities, if such physical and/or mathematical knowledge is available, can provide a clear measure of deviations from the "singular" (integrable) limit. Nevertheless, typically such knowledge will, in fact, be absent (at least until machine-learning techniques improve enough to be able to provide such features; see, e.g., [49] for a recent example). Thus we are faced with the task of potentially exploring a more "generic" and more widely applicable feature that could reveal the relevant conservation laws, their count, and eventually the potential integrability of the nonlinear dynamical system. It is with a view to the latter direction that we now turn to the (full) Lyapunov spectrum of the Salerno lattice.

IV. LYAPUNOV SPECTRUM AND MAXIMAL LYAPUNOV CRITICAL EXPONENT

The existence of chaotic dynamics is one of the indications of nonintegrability [45]. One of the most common tools towards the identification of such chaoticity consists of the maximal (largest) Lyapunov critical exponent (mLCE for short), represented by Λ, of the dynamics associated with the well-known deviation of nearby trajectories. We compute the time evolution of initial perturbations represented by the deviation vector or the tangent map eigenvector χ satisfying [40,50]

$$i\frac{d\chi_n}{dt} = (1+\mu|\psi_n|^2)(\chi_{n+1}+\chi_{n-1}) + \mu(\psi_{n+1}+\psi_{n-1}) \times (\psi_n^*\chi_n + \psi_n\chi_n^*) + \gamma(2|\psi_n|^2\chi_n + \psi_n^2\chi_n^*). \quad (6)$$

We then measure the prototypical diagnostic Λ as follows:

$$\Lambda = \lim_{t\to\infty} L(t), \text{ where } L(t) = \frac{1}{t}\frac{||\chi(t)||}{||\chi(0)||}. \quad (7)$$

To obtain a sense of how this diagnostic varies in the vicinity of integrability, we compute it for a lattice of $N = 100$ particles in Fig. 5. Here we can see that the relevant exponent is generically rather far from the value of $\Lambda \to 0$ and solely tends to it in the immediate vicinity of the integrable limit. In that light, bearing in mind that Hamiltonian systems feature Lyapunov exponents that are pairwise symmetric around 0, if we are aware of such Hamiltonian properties of the system, then the vanishing of this maximal Lyapunov exponent should yield the vanishing of all of them and hence signal the presence of integrability.

Figure 6 shows the finite time mLCE $L(t)$ for different values of N and μ. Here, it can be seen that even though for $N = 3$, the system appears to identify $L(t)$ as tending to 0 with increasing time; the same is clearly not the case for $N = 5$ and beyond, illustrating the nonintegrability of the latter setting. However, more generally, one may not be aware of the Hamiltonian nature of the problem. It may also be desirable to identify the number of conserved quantities of the system. In that vein, we advocate that a relevant numerical tool consists of the calculation of the *full* Lyapunov spectrum λ_i of the system [45]. A systematic prescription to do so was originally discussed in [35,36]. Recently, this was revisited for many-body systems near integrability [23]. It is relevant to remember in that context that the λ_i's corresponding to the conserved quantities are expected to lead to pairs of zeros. Hence, we advocate here the usage of the full Lyapunov spectrum as a generic (i.e., irrespective of the details of the system) and straightforward probe of the number of the system's conservation laws and ultimately a sensitive probe of the dynamical lattice's potential integrability. Since it is known that the ergodic behavior of the system drastically changes as the number of degrees of freedom increases [51,52], we further measure the Lyapunov spectrum as a function of N.

We show the results of the entire Lyapunov spectrum calculation is Fig. 7, which is also a central result of our study. As one expects, the λ_i's are zero at $\mu = 1$ irrespective of

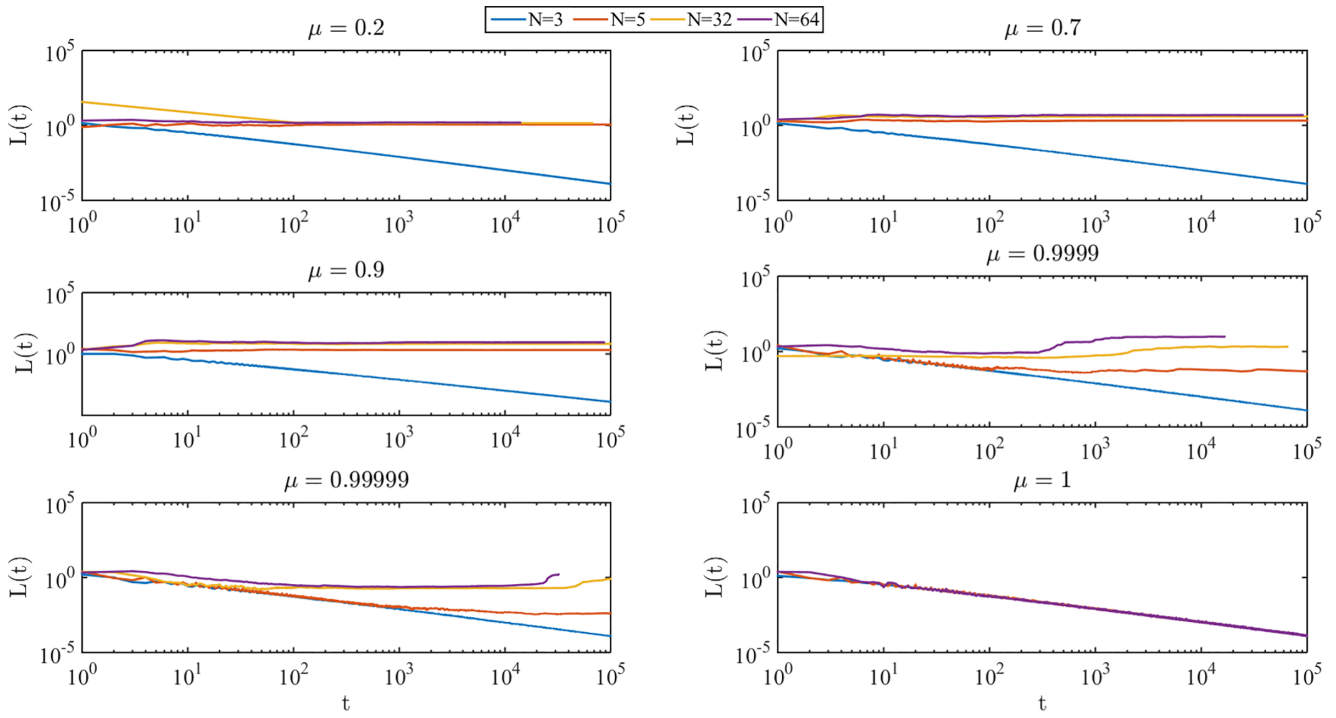

FIG. 6. $L(t)$ in log-log scale for different values of the lattice size N and of the nonlinearity parameter μ obtained from Eq. (7).

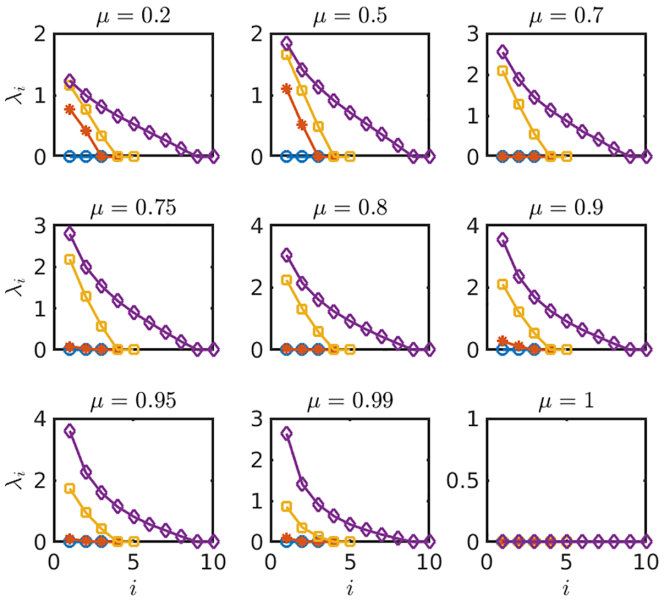

FIG. 7. The positive part of the Lyapunov spectrum, i.e., the positive one-dimensional (1D) Lyapunov exponents λ_i for different values of μ. Here, the number of spectrum components is associated to the x axis, and for each case $i_{total} = N$. The circles, star, square, and diamond symbols represent $N = 3$, $N = 4$, $N = 5$, and $N = 10$, respectively. The Lyapunov spectrum (LS) of the complex wave function associated with the dynamical evolution of the Salerno lattice with N sites, Eq. (1), consists of $2N$ 1D Lyapunov coefficients λ_i, $i = 1, ..., 2N$. Here we consider the N dependence of the LS near and at the integrability limit. We derived the Lyapunov spectrum adopting the procedure described in [45], which is based on the approach of [35,36]. Here we present the positive N Lyapunov coefficients, λ_i, $(i =, 1, 2, ..., N)$.

the number of degrees of freedom. Naturally, this reflects the integrability of the model at this parameter value. Upon deviation from $\mu = 1$, 2 (pairs of), λ_i's remain zero due to the two conserved quantities that are preserved, namely, $\mathcal{H}$ and $\mathcal{A}$ as discussed above, while the rest become nonzero. Recall that the nonvanishing value of the mLCE actually reflects the minimal time (inverse of mLCE) required for the system's chaoticity to manifest itself in connection to its dynamical trajectories. It is important to also note here the role of N, the number of degrees of freedom. When this number is sufficiently low, such as $N = 3$, the limited phase space of the system, in conjunction with the persisting conservation laws, render the recognition of the nonintegrability of the model for $\mu \neq 1$ practically difficult. The same is true, more or less, for $N = 4$, except for parameter values that deviate quite substantially from $\mu = 1$. On the other hand, the example with $N = 5$ and even more demonstrably so the one with $N = 10$ make it clear that only two conserved quantities remain in the evolving dynamics for $\mu \neq 1$, and hence that nonintegrability is now prevalent, even though, of course, these constraints still affect the evolution dynamics.

V. CONCLUSIONS AND FUTURE CHALLENGES

In the present work we have revisited the Salerno model as a vehicle for exploring the deviations from integrability. We have proposed as diagnostics for monitoring such deviations the examination of quantities that are conserved in the integrable limit but whose conservation laws are "broken" as soon as we depart from that limit. Indeed, it was found that

such quantities are sensitive detectors of the deviation from integrability, incurring large variations even for truly minimal departures from the Ablowitz-Ladik case, of the order of 10^{-4}. This illustrates that relevant "former conservation laws" can be used for monitoring such integrability breaking. Nevertheless, we were subsequently faced with the concern that such quantities may not be readily available, unless one has a well-established knowledge of the integrable limit. Hence we sought a set of quantities that could be classified as generic and for which computation methods are well established that could provide us with a count of the relevant conservation laws on and off of the integrable limit. We argued, on the basis of the Salerno example, that the full Lyapunov spectrum is worth considering as a reliable and sufficiently sensitive such set of quantities, certainly past the limit of very small degree-of-freedom systems. Indeed, we recalled that Hamiltonian systems bear Lyapunov exponents in pairs, and each conservation law leads to a pair of such exponents that are vanishing; hence the relevant spectrum is an accurate and (as illustrated in our case example) sensitive monitor of the number of conservation laws in a discrete nonlinear dynamical system such as the Salerno model. Both measurements of the maximal Lyapunov critical exponent for different numbers of degrees of freedom and levels of proximity to integrability and also ones of the full spectrum were shown to be sensitive to such deviations from the integrable limit.

Moving forward, a number of directions for future studies are natural to consider. On the one hand, it seems especially relevant to extend the present analysis to different systems (discrete and continuum) to verify the broader relevance of the conclusions drawn herein in a larger class of corresponding examples. Another direction, however, that is equally or even more promising is that of exploring tools from machine learning to compute corresponding diagnostics in a fast and efficient manner. Indeed, in recent years there has been a substantial effort towards leveraging such tools to identify underlying conservation laws [49] and associated symmetries [53,54]. We believe that the diagnostics proposed herein (such as the identification of the full Lyapunov spectrum) are a natural complement to such efforts, and the utilization of such tools may enable the fast and efficient computation of such diagnostics even for large(r) numbers of degree-of-freedom systems. Such studies are currently in preparation and will be reported in future publications.

ACKNOWLEDGMENTS

This material is based upon work supported by the US National Science Foundation under Grants No. PHY-2110030 and No. DMS-2204702 (P.G.K.), as well as the Ministry of Science, Technological Development and Innovations of the Republic of Serbia, Grants No. 451-03-9/2023-14/20001 and No. 451-03- 68/2023-14/200124 (A.M. and A.M.).

The authors acknowledge insightful discussions with A. Bishop, J. Cuevas, Y. Kevrekidis, A. Saxena, H. Skokos, H. K. Zhang, and W. Zhu on related topics.

[1] G. Gallavotti, *The Fermi–Pasta–Ulam Problem: A Status Report* (Springer-Verlag, Berlin, Germany, 2008).

[2] P. Kevrekidis, Non-linear waves in lattices: Past, present, future, IMA J. Appl. Math. **76**, 389 (2011).

[3] A. J. Sievers and S. Takeno, Intrinsic Localized Modes in Anharmonic Crystals, Phys. Rev. Lett. **61**, 970 (1988).

[4] J. B. Page, Asymptotic solutions for localized vibrational modes in strongly anharmonic periodic systems, Phys. Rev. B **41**, 7835 (1990).

[5] S. Flach and A. V. Gorbach, Discrete breathers – Advances in theory and applications, Phys. Rep. **467**, 1 (2008).

[6] F. Lederer, G. I. Stegeman, D. N. Christodoulides, G. Assanto, M. Segev, and Y. Silberberg, Discrete solitons in optics, Phys. Rep. **463**, 1 (2008).

[7] O. Morsch and M. Oberthaler, Dynamics of Bose–Einstein condensates in optical lattices, Rev. Mod. Phys. **78**, 179 (2006).

[8] M. Sato, B. E. Hubbard, and A. J. Sievers, *Colloquium*: Nonlinear energy localization and its manipulation in micromechanical oscillator arrays, Rev. Mod. Phys. **78**, 137 (2006).

[9] Y. Starosvetsky, K. Jayaprakash, M. A. Hasan, and A. Vakakis, *Dynamics and Acoustics of Ordered Granular Media* (World Scientific, Singapore, 2017)

[10] C. Chong and P. G. Kevrekidis, *Coherent Structures in Granular Crystals: From Experiment and Modelling to Computation and Mathematical Analysis* (Springer, New York, 2018).

[11] M. Remoissenet, *Waves Called Solitons* (Springer-Verlag, Berlin, 1999).

[12] L. Q. English, M. Sato, and A. J. Sievers, Modulational instability of nonlinear spin waves in easy-axis antiferromagnetic chains. II. Influence of sample shape on intrinsic localized modes and dynamic spin defects, Phys. Rev. B **67**, 024403 (2003).

[13] U. T. Schwarz, L. Q. English, and A. J. Sievers, Experimental Generation and Observation of Intrinsic Localized Spin Wave Modes in an Antiferromagnet, Phys. Rev. Lett. **83**, 223 (1999).

[14] P. Binder, D. Abraimov, A. V. Ustinov, S. Flach, and Y. Zolotaryuk, Observation of Breathers in Josephson Ladders, Phys. Rev. Lett. **84**, 745 (2000).

[15] E. Trías, J. J. Mazo, and T. P. Orlando, Discrete Breathers in Nonlinear Lattices: Experimental Detection in a Josephson Array, Phys. Rev. Lett. **84**, 741 (2000).

[16] M. Peyrard, Nonlinear dynamics and statistical physics of DNA, Nonlinearity **17**, R1 (2004).

[17] S. Aubry, Discrete breathers: Localization and transfer of energy in discrete Hamiltonian nonlinear systems, Physica D **216**, 1 (2006).

[18] P. Kevrekidis, *The Discrete Nonlinear Schrödinger Equation*, Vol. 232 (Springer Science & Business Media, New York, 2009).

[19] E. Fermi, J. Pasta, and S. Ulam, Los Alamos Scientific Laboratory Report, LA-1940 (1955).

[20] C. Danieli, D. K. Campbell, and S. Flach, Intermittent many-body dynamics at equilibrium, Phys. Rev. E **95**, 060202(R) (2017).

[21] C. Danieli, T. Mithun, Y. Kati, D. K. Campbell, and S. Flach, Dynamical glass in weakly nonintegrable Klein-Gordon chains, Phys. Rev. E **100**, 032217 (2019).

[22] T. Mithun, C. Danieli, Y. Kati, and S. Flach, Dynamical Glass and Ergodization Times in Classical Josephson Junction Chains, Phys. Rev. Lett. **122**, 054102 (2019).
[23] M. Malishava and S. Flach, Lyapunov Spectrum Scaling for Classical Many-Body Dynamics Close to Integrability, Phys. Rev. Lett. **128**, 134102 (2022).
[24] N. J. Zabusky and M. D. Kruskal, Interaction of "Solitons" in a Collisionless Plasma and the Recurrence of Initial States, Phys. Rev. Lett. **15**, 240 (1965).
[25] M. A. Porter, N. J. Zabusky, B. Hu, and D. K. Campbell, Fermi, Pasta, Ulam and the birth of experimental mathematics, Am. Sci. **97**, 214 (2009).
[26] M. Ablowitz and H. Segur, *Solitons and the Inverse Scattering Transform* (SIAM, Philadelphia, 1981), Vol 4.
[27] M. Ablowitz, *Nonlinear Dispersive Waves, Asymptotic Analysis and Solitons* (Cambridge University Press, Cambridge, 2011).
[28] Y. S. Kivshar and B. A. Malomed, Dynamics of solitons in nearly integrable systems, Rev. Mod. Phys. **61**, 763 (1989).
[29] D. Hennig, N. I. Karachalios, and J. Cuevas-Maraver, The closeness of localized structures between the Ablowitz–Ladik lattice and discrete nonlinear Schrödinger equations: Generalized AL and DNLS systems, J. Math. Phys. **63**, 042701 (2022).
[30] D. Hennig, N. I. Karachalios, and J. Cuevas-Maraver, The closeness of the Ablowitz-Ladik lattice to the discrete nonlinear Schrödinger equation, J. Differ. Equations **316**, 346 (2022).
[31] S. V. Dmitriev, P. G. Kevrekidis, B. A. Malomed, and D. J. Frantzeskakis, Two-soliton collisions in a near-integrable lattice system, Phys. Rev. E **68**, 056603 (2003).
[32] M. Salerno, Quantum deformations of the discrete nonlinear Schrödinger equation, Phys. Rev. A **46**, 6856 (1992).
[33] M. Ablowitz and J. Ladik, Nonlinear differential–difference equations and Fourier analysis, J. Math. Phys. **17**, 1011 (1976).
[34] M. J. Ablowitz, B. Prinari, and A. D. Trubatch, *Discrete and Continuous Nonlinear Schrödinger Systems*, London Mathematical Society Lecture Note Series (Cambridge University Press, Cambridge, England, 2003).
[35] G. Benettin, L. Galgani, A. Giorgilli, and J.-M. Strelcyn, Lyapunov characteristic exponents for smooth dynamical systems and for Hamiltonian systems, A method for computing all of them. Part 1: Theory, Meccanica **15**, 9 (1980).
[36] G. Benettin, L. Galgani, A. Giorgilli, and J. Strelcyn, Lyapunov characteristic exponents for smooth dynamical systems, A method for computing all of them. Part 2: Numerical application, Meccanica **15**, 21 (1980).
[37] C. Skokos, The Lyapunov characteristic exponents and their computation, in *Dynamics of Small Solar System Bodies and Exoplanets*, edited by J. J. Souchay and R. Dvorak (Springer Berlin Heidelberg, 2010), pp. 63–135.
[38] D. Cai, A. R. Bishop, and N. Grønbech-Jensen, Perturbation theories of a discrete, integrable nonlinear Schrödinger equation, Phys. Rev. E **53**, 4131 (1996).
[39] J. Gómez-Gardeñes, F. Falo, and L. Floria, Mobile localization in nonlinear Schrödinger lattices, Phys. Lett. A **332**, 213 (2004).
[40] T. Mithun, A. Maluckov, B. M. Manda, C. Skokos, A. Bishop, A. Saxena, A. Khare, and P. G. Kevrekidis, Thermalization in the one-dimensional Salerno model lattice, Phys. Rev. E **103**, 032211 (2021).
[41] A. C. Cassidy, Chaos and thermalization in the one-dimensional Bose-Hubbard model in the classical-field approximation, arXiv:1003.5206.
[42] D. Cai, A. R. Bishop, N. Grønbech-Jensen, and B. A. Malomed, Moving solitons in the damped Ablowitz-Ladik model driven by a standing wave, Phys. Rev. E **50**, R694 (1994).
[43] V. Caudrelier and N. Crampé, New integrable boundary conditions for the Ablowitz-Ladik model: From Hamiltonian formalism to nonlinear mirror image method, Nucl. Phys. B **946**, 114720 (2019).
[44] D. Cai, A. R. Bishop, and N. Grønbech-Jensen, Localized States in Discrete Nonlinear Schrödinger Equations, Phys. Rev. Lett. **72**, 591 (1994).
[45] A. J. Lichtenberg and M. A. Lieberman, *Regular and Chaotic Dynamics*, Applied Mathematical Sciences Vol. 38 (Springer, New York, 1992).
[46] Freely available from http://www.unige.ch/~hairer/software.html.
[47] E. Hairer, S. P. Nørsett, and G. Wanner, *Solving Ordinary Differential Equations, I. Nonstiff Problems*, 2nd ed., Springer Series in Computational Mathematics Vol. 14 (Springer, New York, 1993).
[48] C. Danieli, B. M. Manda, T. Mithun, and C. Skokos, Computational efficiency of numerical integration methods for the tangent dynamics of many-body Hamiltonian systems in one and two spatial dimensions, Math. Eng. **1**, 447 (2019).
[49] Z. Liu and M. Tegmark, Machine Learning Conservation Laws from Trajectories, Phys. Rev. Lett. **126**, 180604 (2021).
[50] T. Mithun, Y. Kati, C. Danieli, and S. Flach, Weakly Nonergodic Dynamics in the Gross-Pitaevskii Lattice, Phys. Rev. Lett. **120**, 184101 (2018).
[51] J.-P. Eckmann and D. Ruelle, Ergodic theory of chaos and strange attractors, Rev. Mod. Phys. **57**, 617 (1985).
[52] T. Mithun, C. Danieli, M. V. Fistul, B. L. Altshuler, and S. Flach, Fragile many-body ergodicity from action diffusion, Phys. Rev. E **104**, 014218 (2021).
[53] Z. Liu and M. Tegmark, Machine Learning Hidden Symmetries, Phys. Rev. Lett. **128**, 180201 (2022).
[54] R. Bondesan and A. Lamacraft, Learning symmetries of classical integrable systems, arXiv:1906.04645.